Operation of a prototype Microgrid system based on micro-sources equipped with fast-acting power electronics interfaces

D. Georgakis[1] dimgeo@mail.ntua.gr
S. Papathanassiou[1] st@power.ece.ntua.gr
N. Hatziargyriou[1] nh@power.ece.ntua.gr
A.Engler[2] aengler@iset.uni-kassel.de
Ch. Hardt[3] Christian.Hardt@SMA.de

[1]. National Technical University of Athens (NTUA), Greece
[2]. Institut für Solare Energieversorgungstechnik (ISET), Kassel, Germany
[3]. SMA Regelsysteme GmbH, Niestetal, Germany

***Abstract*— The paper presents experimental results from the operation of a prototype Microgrid system, installed in the National Technical University of Athens, which comprises a PV generator, battery energy storage, local load and a controlled interconnection to the LV grid. Both the battery unit and the PV generator are connected to the AC grid via fast-acting DC/AC power converters. The converters are suitably controlled to permit the operation of the system either interconnected to the LV network, or in stand-alone (island) mode, with a seamless transfer from the one mode to the other. The paper provides a technical description of the system components and the control concept implemented, along with extensive measurement results which demonstrate its capability to operate in the aforementioned way.**

I. INTRODUCTION

The penetration of distributed generation resources to the low voltage grids, such as photovoltaics, CHP micro-turbines, small wind turbines in certain areas and fuel cells in the near future, is constantly increasing, altering the traditional operating principle of the grids. A particularly promising aspect, related to the proliferation of small-scale decentralized generation, is the possibility for parts of the network comprising sufficient generating resources to operate in isolation from the main grid, in a deliberate and controlled way. Grid portions with such a capability are called Microgrids ([1]).

A critical factor in order to exploit the potential offered by the microgrid concept is the presence of micro-sources, with fast-acting power electronics interfaces to regulate voltage and frequency and ensure proper load sharing among the various sources, when operating in isolated mode. In interconnected mode, the micro-source and central micro-grid controllers regulate the power exchange with the grid, monitor grid conditions and ensure proper separation. Micro-source controllers suitable for this task are being developed (e.g. [2,3]) and implemented in inverters, which could support the operation of microgrids.

In the paper, a prototype, laboratory-scale microgrid is presented, which comprises a PV generator, battery energy storage, local load and a controlled interconnection to the public LV grid. Its objective is to explore control concepts and operating policies and demonstrate the feasibility of the microgrid concept. The existing system is already capable of operating in stand-alone and grid-connected mode, with a seamless transition from one state to the other, as demonstrated by measurements included in this paper.

II. THE EXPERIMENTAL MICROGRID SYSTEM

A. System description

The composition of the microgrid system is shown in Figure 1, along with a photo of the actual installation. It is a modular system, comprising a PV generator as the primary source of power. The addition of a small WT is also planned for the immediate future. Both microsources are interfaced to the 1-phase AC bus via DC/AC PWM inverters. A battery bank is also included, interfaced to the AC system via a bi-directional PWM voltage source converter. The microgrid is connected to the local LV grid, as shown in Figure 2.

Fig. 1. The laboratory microgrid system

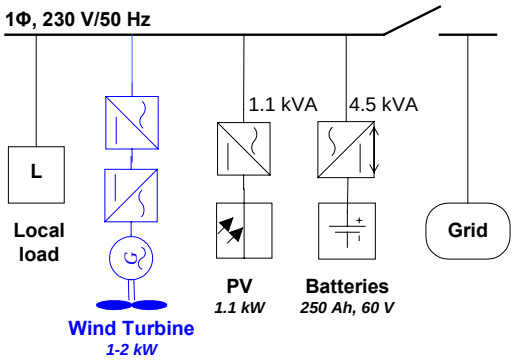

Fig. 2. Schematic diagram of microgrid system (possible WT or other distributed source extension).

When the system is connected to the grid, the local load receives power both from the grid and the local micro-sources. In case of grid power interruptions, the microgrid can transfer smoothly to island operation and subsequently reconnect to the public grid.

The central component of the microgrid system is the battery inverter, which regulates the voltage and frequency when the system operates in island mode, taking over the control of active and reactive power. The battery unit power electronics interface, schematically illustrated in Figure 3, consists of a Cuk DC/DC converter and a voltage source PWM inverter, both bi-directional, permitting thus charging and discharging of the batteries. The DC/DC converter provides the constant 380 V DC voltage to the DC/AC converter input. It is a bi-directional topology with buck and boost capabilities. This is required because of the big variations of the battery voltage. The HF transformer, operating at 16.6 kHz, provides electrical isolation between the battery bank and the grid. The four-quadrant DC/AC converter comprises a single phase IGBT bridge, output filters and a grid-connection inductor.

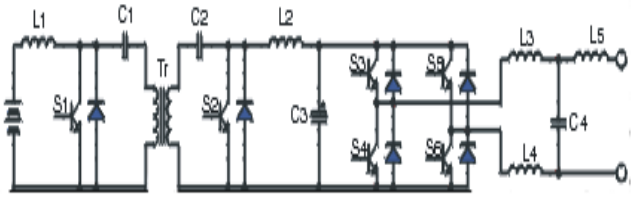

Fig. 3. Power section of the battery inverter, [4].

The battery inverter operates in voltage control mode (regulating the magnitude and phase/frequency of its output voltage), acting as a "grid-forming" unit, when the microgrid operates in island mode, i.e. setting the voltage and frequency of the system. When the microgrid operates in parallel to the grid, in which case the latter defines the operating frequency and voltage, the inverter acts as a "grid-following" unit, though the control mode is not changed.

The PV inverter performs the MPPT function of the photovoltaic generator and operates as a "grid-parallel" unit, responsible for maximizing the PV power output, but without any participation in the voltage or frequency regulation. In fact, it is a current source, characterized by a high impedance, thus not affecting the grid.

B. Principle of control

A microgrid where multiple energy sources and storage facilities (such as batteries) are present, resembles in many ways an electric power system, where multiple generators participate in the frequency and voltage regulation and all share the total active and reactive power demand. This function is primarily performed by the speed governors and the voltage regulators of the individual units, depending on their active power-frequency and reactive power – voltage control characteristics. These characteristics are known as "droop curves" and are schematically illustrated in Figure 4. Each one is defined by two basic quantities:

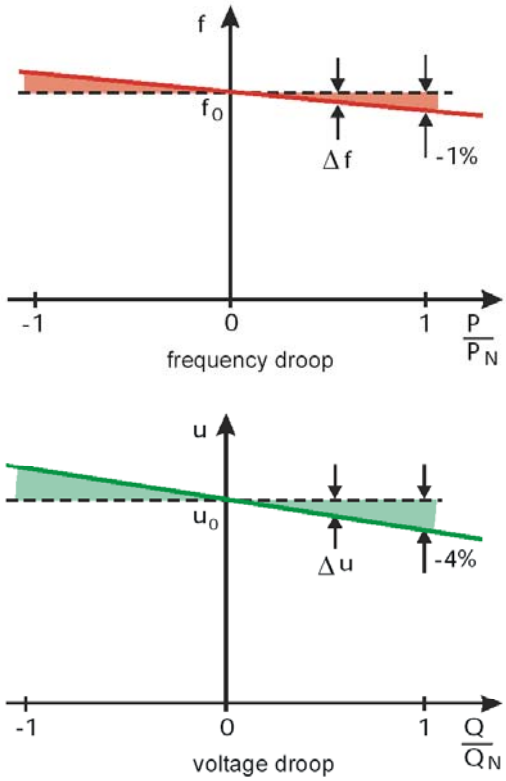

Fig. 4. Grid compatible frequency and voltage droops.

· The "idle" frequency and voltage, f_o and u_o, corresponding to the value of the frequency or voltage when the active, resp. reactive, output power is zero.

· The "droop" value, i.e. the slope $\Delta f/\Delta P$ and $\Delta V/\Delta Q$, denoting the difference in output frequency or voltage, between no-load and full-load operation of the device.

When a single unit feeds the microgrid, its frequency and voltage is directly determined by its droop curve, depending on its active and reactive power output. If multiple sources operate within the same system, no single unit regulates the frequency, but they all contribute by sharing the load power according to their individual droop curves.

This principle has been directly transferred to the control of battery inverters ([2]), as well as other micro-sources capable of regulating their active and reactive power output. Hence, each battery inverter unit, primarily a voltage source inverter with regulated AC voltage magnitude and frequency, is controlled according to the characteristics of Figure 4. Thus, proper load sharing is ensured (e.g. [3]) and frequency regulation is achieved in island mode, whereas potential problems with large reactive currents circulating between the distributed sources are avoided. In grid-interconnected mode, where frequency and voltage are practically fixed, the settings of the droop curve parameters determine the active and reactive output power of each inverter. For the microgrid, a central supervisory control system also exists, which is capable of altering the individual inverter settings in real-time.

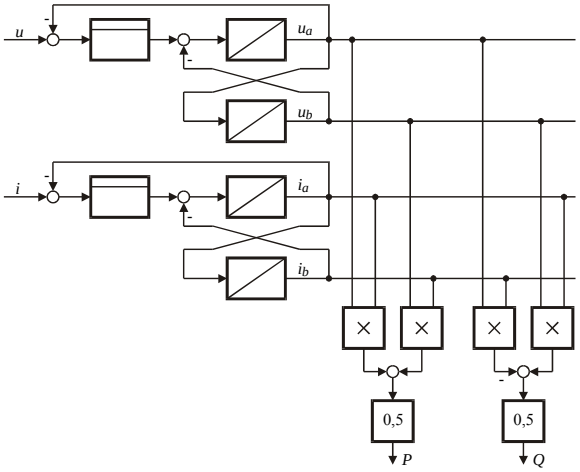

Fig. 5. Fast single-phase *P*/*Q*-computation

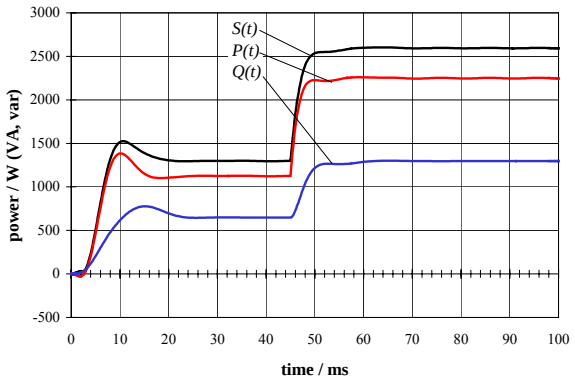

Fig. 6. Example for single-phase *P*/*Q*-acquisition (simulation)

C. *Computing active and reactive power*

The above outlined control approach is based on (fast) instantaneous active and reactive power values, which are especially difficult to obtain in single phase systems. Here it is necessary to determine the complex apparent power $\underline{S}$. This can be described with the space vector of the voltage and current:

$$\underline{S} = P + jQ = \frac{1}{2}\underline{u} \cdot \underline{i}^* = \frac{1}{2}(u_a + ju_b)(i_a - ji_b) \cdot$$

Splitting up the complex apparent power $\underline{S}$ into its real and imaginary part results in the wanted functions for the instantaneous active power *P* and reactive power *Q*:

$$P = \frac{1}{2} \cdot (u_a \cdot i_a + u_b \cdot i_b)$$

$$Q = \frac{1}{2} \cdot (u_b \cdot i_a - u_a \cdot i_b) \cdot$$

The corresponding block diagram is depicted in Figure 5. A special filter is used for calculating the orthogonal components *a* and *b* of the voltage and the current [5]. An example for the single-phase *P*/ *Q* acquisition is depicted in Figure 6. The change of the power is detected within 7 ms.

The main advantages of this patented approach are:

- no zero crossing detection is required,
- the computation of active and reactive power of the fundamental frequency within one period and
- the simplicity of the algorithm.

III. EXPERIMENTAL RESULTS

The results presented in this section have been recorded during the testing phase of the system, after the recent upgrade of its controllers, to include the droop characteristics described in the previous paragraph.

In Figure 7, a sequence is shown where the operating mode of the microgrid changes from island to grid-interconnected and then back to island mode. The three diagrams illustrate the frequency and voltage of the microgrid and the public LV grid, as well as the active power of the battery inverter, the PV generator, the local load and the grid (positive when flowing into the microgrid).

Initially the system is disconnected from the grid, feeding a local load of 0.5 kW. The PV power is gradually increasing, from 150 to 200 W, whereas the battery inverter output is correspondingly decreasing from 300 to 250 W. Due to the negative frequency droop, this causes a gradual increase of the frequency in the islanded part. The voltage on the other hand remains practically constant, since no significant change of the reactive power occurs.

At approximately 200 sec, the microgrid is synchronized to the grid and its frequency and voltage become equal to the values of the network (f~50.05 Hz, V~235 V). The "idle" frequency fo of the inverter was set to 50.05 Hz, causing thereby the inverter active power to approach zero. At approximately 400 s, the microgrid is disconnected from the grid (deliberate disconnection, without any grid failure event) and returns to its initial operating state. During the transition from isolated to interconnected mode and vice versa, the PV and load continue to operate without any interruption or other disturbance.

The synchronization transients, which are not shown in Figure 7, due to the sampling of rms quantities at a low rate (1 Hz), are illustrated in Figure 8. In diagram 8(a) the grid current is shown, which exhibits a maximum value of approximately 5.5 Arms, i.e. less than 30% of the battery inverter rated current (the non-zero current before synchronization in diagram 8(a) is due to the quantization error of the measuring device). The two voltages on the terminals of the synchronization contactor (microgrid and grid side) are included in diagram 8(b). In the first 0.3 s the phase difference between the island and grid voltages is gradually decreasing, until synchronization conditions are fulfilled (at about 0.3 s). Subsequently, the system operates at a single voltage and frequency.

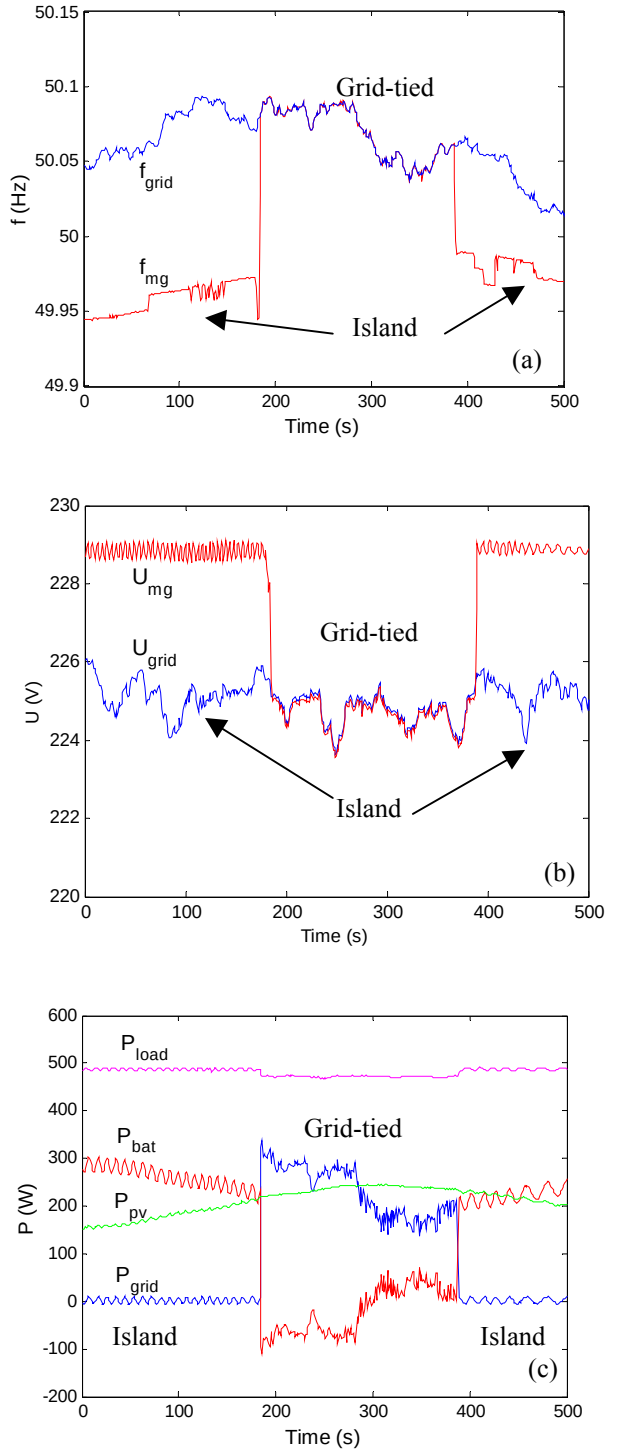

Fig. 7. Successive changes of the microgrid operating mode, from island to interconnected and vice-versa. (a) Frequency, (b) Voltage and (c) Power of the components and the grid

Using measurements performed over a longer time interval, the implementation of the frequency and voltage droops has been tested. This is illustrated in Figures 9 and 10, where a large number of measurement points have been plotted on the same axes with the specific control characteristics, which were programmed in the battery inverter for the measurement interval. Notably, the

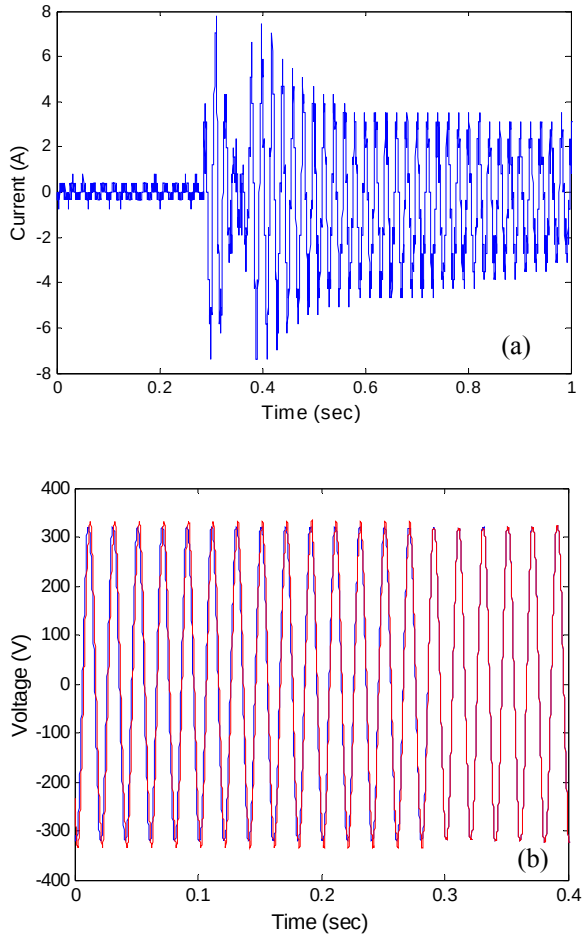

Fig. 8 Synchronization to the grid. (a) Current on the grid-tie, (b) Grid (blue) and microgrid (red) voltages.

measurement interval comprises autonomous operation periods, with varying solar radiation and load levels.

In the first diagram of Figure 9 the frequency vs. the active power is plotted. These measurements correspond to three intervals where the battery inverter was programmed with different "idle" frequency values (f_o=49,50,51 Hz respectively), but the same "droop" value (-1 Hz/P_{nom}). It is apparent that the frequency regulation loop performs as intended, closely tracking the droop characteristic implemented in the inverter controller.

Similarly, in the second diagram of Figure 9, the inverter terminal voltage vs. reactive power plot is shown. The voltage measurements correspond to two different "idle" voltage values (V_o=220 and 230 V) for the battery inverter, while the "droop" value is the same (-6%/Q_{nom}) in both cases. The voltage regulation loops track correctly the droop characteristic when the reactive power is positive (inductive load), but less so for capacitive loading of the inverter, in which case the slope appears somewhat increased.

Similar remarks apply for the diagrams of Figure 10, where plots are shown for different slopes ("droop" values) of the control characteristics.

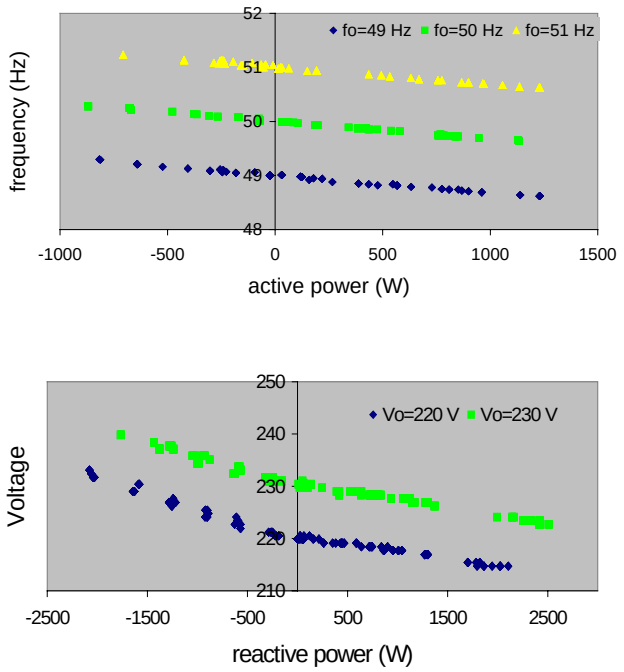

Fig. 9. Inverter frequency and terminal voltage vs active and reactive power respectively.

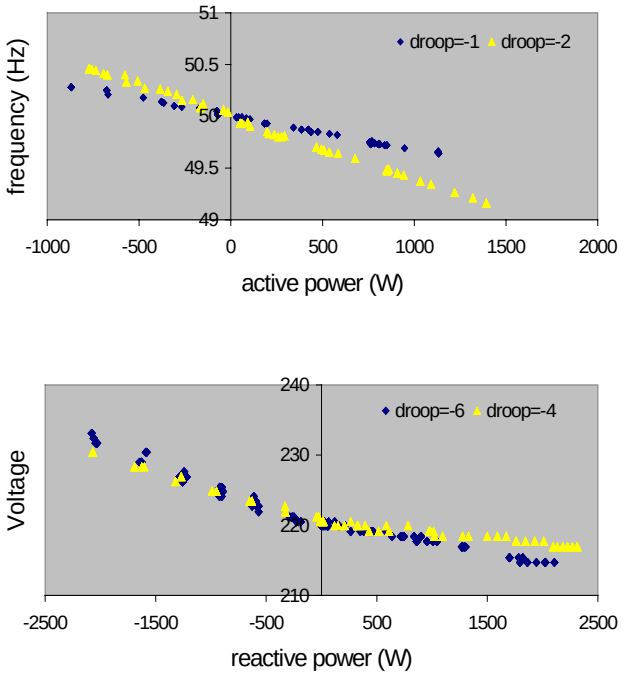

Fig. 10. The effect of changes in the frequency and voltage droop values.

An example in the time domain of the effect from changing the idle frequency, f_o, of the battery inverter is illustrated in Figure 11. The microgrid operates in grid-tied mode and therefore its frequency is practically fixed by the grid, at approximately 50Hz. Due to the control concept implemented, the inverter output power is determined by its

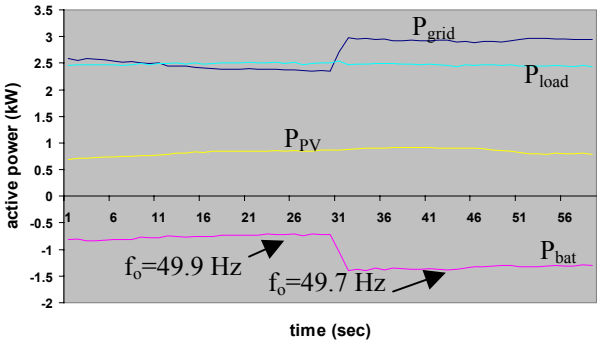

Fig. 11 The effect of the f_o change on the power sharing

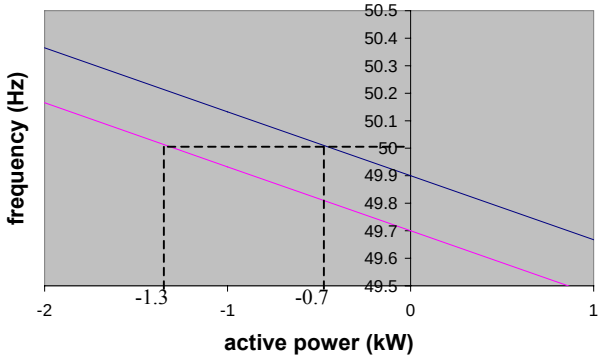

Fig. 12. The effect of the f_o change on the inverter output power.

frequency droop characteristic, as shown in Figure 12. The idle frequency f_o initially is set to 49.9 Hz, resulting in the inverter absorbing 0.7 kW from the grid (charging the batteries). At about 30 sec, f_o changes to 49.7 Hz, corresponding to the second control characteristic in Figure 12. According to this characteristic, for the given grid frequency (equal to 50 Hz at the instant of the change), the inverter active power has to change to approximately 1.3 kW, as it is confirmed by the measurement in Fig. 11. Since the PV and load powers remain constant, this change is directly reflected on the power drawn from the grid.

IV. CONCLUSION

The paper presents an assessment of the operation of a laboratory microgrid, incorporating micro-sources and local loads. First a description of the system components and the control principles implemented is given. Then experimental results are provided which demonstrate the capability of the system to operate either in parallel to the grid or in autonomous mode. The transition from one state to the other is performed seamlessly, without any interruption or other disturbances to the micro-sources and the load of the microgrid.

ACKNOWLEDGMENT

The work presented in the paper has been performed within the framework of the EU research project NNE5-2001-00463 "MICROGRIDS". The authors gratefully acknowledge the support received from the EU for their research.

REFERENCES

[1] R. Lasseter, A. Akhil, C. Marnay, J. Stephens, J. Dagle, R. Guttromson, A. S. Meliopoulos, R. Yinger and J. Eto, "White Paper on Integration of Distributed Energy Resources – The CERTS MicroGridConcept". LBNL-50829, Office of Power Technologies of the US Department of Energy, Contract DE-AC03-76SF00098, April 2002.

[2] Alfred Engler, Regelung von Batteriestromrichtern in modularen und erweiterbaren Inselnetzen, Ph.D. dissertation, Univ. of Kassel, 2002, publisher Dissertation.de, ISBN 3-89825-439-9

[3] Ph. Strauss, A. Engler, "AC coupled PV hybrid systems and Microgrids – State of the Art and Future Trends". 3rd World Conference on Photovoltaic Energy Conversion, Osaka, Japan, May 2003.

[4] "Sunny Island – Installation and Operating Instructions. Bidirectional Battery Inverter SI3300 for stand-alone applications, V.2.1 (preliminary)". SMA Regelsysteme GmbH.

[5] B. Burger, A. Engler,"Fast Signal Conditioning in Single Phase Systems", EPE, Graz, 08/2001